

Energy management in distribution systems, considering the impact of reconfiguration, RESs, ESSs and DR: A trade-off between cost and reliability

Ehsan Hooshmand, Abbas Rabiee*

Department of Electrical Engineering, University of Zanjan, Zanjan, Iran

ARTICLE INFO

Article history:

Received 21 August 2018

Received in revised form

9 February 2019

Accepted 17 February 2019

Available online 21 February 2019

Keywords:

Distribution system reconfiguration (DSR)

Demand response (DR)

Cost of Energy not supplied (CENS)

Wind turbine (WT)

Photo-voltaic (PV)

Energy storage system (ESS)

ABSTRACT

The distribution network operator is usually responsible for improvement of efficiency and reliability of the network. This paper proposes a framework to demonstrate the impact of renewable energy sources (RESs), energy storage systems (ESSs), demand response (DR) and reconfiguration on the optimal sharing of energy. The proposed model determines the optimal locations of RESs, ESSs and DR in the distribution network to minimize simultaneously the cost of energy procurement and energy not supplied. A multi-objective optimization problem is formulated with a mixed-integer second-order cone programming model and ϵ -constraint method is used to generate Pareto optimal solutions. The network reconfiguration is also considered to optimize the power flow by changing the network topology. The proposed model is implemented on the IEEE standard 33-bus radial test system, and solved by General Algebraic Modeling System (GAMS) optimization software. According to the simulation results, the proposed framework is beneficial both from the reliability and economic perspectives.

© 2019 Elsevier Ltd. All rights reserved.

1. Introduction

1.1. Background and motivations

In recent years, application of distributed energy resources such as wind, solar etc, has been increased to reinforce the distribution systems (DSs) from different aspects such as better reliability, higher power quality, voltage profile enhancement, total cost minimization, etc. On the other hand, distributed generations (DGs) such as photo-voltaic (PV), wind turbine (WT) and energy storage system (ESS) are expected to play an important role in future electricity supply and low cost energy systems. A DS, however, is relatively less expensive than a transmission system and the outages in a typical DS have usually localized effects [1]. However, being reported that the DS is the main contributor to the unavailability of energy supply to the end-users, significant attention should be paid to its reliability enhancement [2]. The objective of reliability improvement of DSs stands for the reduction of the frequency and duration of energy interruptions that affect the

customers [3]. This is generally achieved through network automation, efficiently designed protection schemes, proper re-closing and switching, fault prediction techniques, efficiently organized and fast repair teams and the improvement of the dependability of single components [4]. Using optimal placement of energy generation/management options such as WT, PV, ESS and DR as well as DS reconfiguration (DSR), the unnecessary active power flow in distribution feeders will be reduced.

1.2. Literature survey

According to the existing literature, numerous scientific works have been proposed to see different features of optimal WT, PV, ESS and DR placement and scheduling under different loading conditions by considering different objectives. The current literature, mainly focused on traditional objectives. For example, in Ref. [5] particle swarm algorithm and fuzzy-based optimization technique are proposed to minimize the operation cost and the net emission, simultaneously. In Ref. [6], optimal DR and ESS scheduling is studied to minimize the loss payment. A new particle swarm optimization is proposed in Ref. [7] in order to determine the optimal DG locations, size, and the contract price of the DGs' generated power. The proposed method seeks to voltage profile

* Corresponding author.

E-mail addresses: E.hooshmand@znu.ac.ir (E. Hooshmand), rabiee@znu.ac.ir (A. Rabiee).

Nomenclature*Sets & Indices*

i	Index for network buses
l	Index for network feeders
t	Index for operation intervals
Ω_l	Set of lines in distribution network
Ω_{ESS}	Set of nodes containing ESS
Ω_{DR}	Set of nodes participating in demand response
Ω_n	Set of all network nodes
Ω_t	Set of time periods

Variables

EPC	Energy procurement Cost (\$)
CENS	Cost of Energy Not Supplied (\$)
ENS_t	Energy Not Supplied at time period t
$(P/Q)_{i,t}^G$	Active/reactive power generation in node i at time period t
$(P/Q)_{i,t}^W$	Active/reactive power injection of node i at time period t with WT
$(P/Q)_{i,t}^P$	Active/reactive power injection of node i at time period t with PV
$(P/Q)_{i,t}^{D/G}$	Active/reactive demand of node i at time period t with demand response
z_i^{ESS}	Binary decision variable for installation of ESS at node i
z_i^{DR}	Binary decision variable indicating whether node i participates in DR or not
z_i^W	Binary decision variable for installation of WT at node i
z_i^P	Binary decision variable for installation of PV at node i
z_i^f	Binary decision variable to model the on/off status of feeder l
$P_{i,t}^{ch/dch}$	Charge/discharge power of ESS at node i at time period t
$ES_{i,t}$	Energy stored in ESS at node i at time period t
$(P/Q)_{i,t}^{net}$	Net active/reactive power injection to node i at time period t with demand response
$I_{l,t}$	Current flowing through the line l at time t
$V_{i,t}$	Voltage magnitude at node i at time t (pu)
$\xi_{i,t}$	Demand response decision variable of node i at time period t

Parameters

U_l	Average repair time of branch l [h]
λ_l	Failure rate of branch l [failures/year]
$VOLL_t$	Value of lost load at time t
κ_t	Pool market price at time t in day ahead market (\$/MWh)
MN^{ESS}	Maximum number of nodes allowed to install the ESS
MN^{DR}	Maximum number of nodes allowed to participate in demand response
MN^W	Maximum number of nodes allowed to install the wind plant
MN^P	Maximum number of nodes allowed to install the PV
$V^{min/max}$	Maximum/minimum voltage magnitude
I_l^{max}	Maximum feeder of l capacity
$ES_i^{max/min}$	Maximum/minimum energy stored at node i
$P_i^{ch,max/min}$	Maximum/minimum power charge of ESS at node i
$P_i^{dch,max/min}$	Maximum/minimum power discharge of ESS at node i
$\eta_{ch/dch}$	Efficiency of charging and discharging of ESS (%)
$(P/Q)_{i,t}^{DO}$	Initial active/reactive demand of node i at time period t without demand response
$\chi_i^{-/+}$	coefficients for modeling the lower/upper limits of Wind plant reactive power outputs
$\Phi_t^{w/p}$	Forecasting output of WT & PV at time period t (%)
$\Lambda^{w/p}$	Rated active power of WT & PV connected to node i
$\xi_i^{max/min}$	Maximum/minimum demand flexibility at node i
R_l	Resistance of line l
X_l	Reactance of line l

Abbreviations

DSR	Distribution system reconfiguration
DG	Distributed generation
DR	Demand response
CENS	Cost of Energy not supplied
WT	Wind turbine
EPC	Energy procurement cost
LFB	Line flow-based
MISO	Midcontinent independent system operator
DNO	Distribution network operator
RES	Renewable energy source
PV	Photo-voltaic
ESS	Energy storage system
VOLL	Value of lost load
ORESA-DSR	Optimal RES allocation and DS reconfiguration

and stability improvement, loss reduction, and reliability enhancement. A novel energy storage system was also proposed in Ref. [8] to achieve cost reduction in hardware manufacturing and efficiency improvement. The method proposed in Ref. [9] finds the optimal size and location of wind farms (WFs) based on a sensitivity analysis to improve voltage stability margin. As it can be seen, some traditional objective functions such as active/reactive power losses, voltage deviation and total cost have been the main focus of all above works.

DSR is to modify the topological structure of distribution feeders by changing open/closed status of sectionalizing switches. This is an effective tool to improve the operational indices of DSRs, such as power loss reduction [10], load balancing [11], etc. The

quantification of reliability in order to be considered as an objective has been studied in several researches. According to the literature [2–4], the DSR with respect to enhancement of reliability emerges as a promising operational strategy to be considered together with the aforementioned aims, both in planning and operation phases.

It is desirable to use an AC power flow model in power system operation and planning problems [12], since it is well capable to precisely describe the real power system behavior. However, an operation or planning problem based on AC power flow constraints is formulated as a non-convex and nonlinear optimization problem. Its computation burden is huge and only local optimal solutions could be found. Therefore, AC power flow-based models may not be suitable for large-scale systems with considerable uncertainties of

renewable energies. The unit commitment model which is currently solved in midcontinent independent system Operator (MISO) cannot reach a zero optimality gap even using linear optimization models, let alone using the nonlinear optimization models [13]. On the other hand, the DC power flow models have been proposed and widely used for power system planning, which is formulated as a mixed integer programming model and can be efficiently solved by commercial solvers. But, the DC models ignore the reactive power balance, voltage magnitude constraints and power losses [14]. As an alternative AC model, line flow-based (LFB) model has been proposed in Ref. [15]. The LFB model directly uses bus voltage magnitudes and line power flows as independent variables and thus the power loss and voltage can be effectively considered. The LFB model has also a good convergence characteristic and computational efficiency, which make it favorable for large-scale nonlinear and mixed integer models related to operation and planning of DSs. In this context, in Ref. [16] a convex model for active distribution network planning is proposed by integration of ESSs. In Ref. [17], an active distribution network planning model is presented by incorporating PV inverter control schemes without inclusion of ESSs. Also [18], presents a convex optimization model for distributed energy storage planning and operation. In Ref. [19], a second order conic programming (SOCP) model is proposed based on the information gap decision theory (IGDT) to maximize load pickup considering the uncertainty of load increment. Recently, several methods have been proposed to convexify the OPF [16–20].

Recently, Demand response (DR) or load flexibility has been offered as a dependable resource option for balancing supply and demand [21]. According to the definition by US department of energy, “DR provides an opportunity for consumers to play a significant role in the operation of the electric grid by reducing or shifting their electricity usage during peak periods in response to time-based rates or other forms of financial incentives”.

Various applications of DR are outlined in Refs. [21,22]. Di Somma et al. in Ref. [23], presented a stochastic programming model for the optimal scheduling of distributed energy resources. The main aim of the study is to reduce energy cost and CO₂ emission while, satisfying time-varying user demand. The potential of demand response on isolated hybrid renewable energy systems, in order to optimize the system’s dispatch by minimizing the operation costs and the peak demand is analysis in Ref. [24]. In Ref. [25], an analysis has been performed on the effects of DR on voltage profile improvement during peak loading condition and loss reduction in distribution networks. Also [26], addresses the application of DR at PV-penetrated DSs. However, most previous works have not considered the impact of DR on DSR. Table 1 is a summary

of the existing literature and differences between them and the state of the art.

1.3. Contributions

This paper presents a multi-objective energy management model for DSs while considering the cost of energy not supplied (CENS) and energy procurement cost (EPC) as competitive objectives, which reflect the reliability and economic perspectives of DSs. DSR is employed along with WTs, PVs, ESSs and DR participation to optimize the energy consumption in the network for a given operation horizon. The proposed optimal RES allocation and DS reconfiguration (ORESAs-DSR) model is formulated as a mixed-integer second order cone programming (MISOCP) problem, which is convex and computationally efficient. The gap that this paper tries to fill is how the combination of DR, RESs, ESSs and DSR can reduce the EPC and CENS, simultaneously.

1.4. Paper organization

The rest of this paper is organized as follows: Section 2 discusses the proposed ORESAs-DSR model. The detailed description of the proposed convex optimization model is presented in this section. In Section 3 the case study and a comprehensive sensitivity analysis is done to investigate different aspects of the proposed ORESAs-DSR model. Finally, the paper conclusions are outlined in Section 4.

2. Description of the proposed ORESAs-DSR model

2.1. Basic concept of the proposed model

The proposed ORESAs-DSR model provides a convex optimization model with an optimal global solution. The developed ORESAs-DSR will make it possible for the distribution network operator (DNO) to adequately schedule the energy supply sources, with a variety of options such as RESs and consumer participation in the context of DR program. The concept of the proposed ORESAs-DSR model is illustrated in Fig. 1. Given that DNO schedules for a 24-h period, according to Fig. 1, the inputs are the forecasts of DGs available capacity and load demand. Based on the input values of load forecast data [6], and the forecast data of PV/WT available capacity [22,30], the outputs of the proposed ORESAs-DSR framework are the optimal allocation (placement and schedule) of a variety of renewable resources, the demand response program and the optimal topology of the network.

Table 1
Comparison of existing literature with the proposed model.

Reference	Non-convex model	convex model	DSR	DG	ESS	DR	Reliability maximization	EPC or Loss minimization
[2–4]	✓		✓				✓	✓
[5,27]	✓			✓	✓			✓
[6,22]	✓			✓	✓	✓		✓
[7]	✓			✓			✓	✓
[9]	✓			✓				✓
[10,11]	✓		✓					✓
[12,28]	✓							✓
[16]		✓	✓	✓	✓			✓
[18]		✓		✓	✓			✓
[19]		✓					✓	
[29]		✓		✓				
[20]		✓				✓		✓
[23,24,26,30]	✓		✓		✓		✓	
[31]	✓					✓		
Proposed		✓	✓	✓	✓	✓	✓	✓

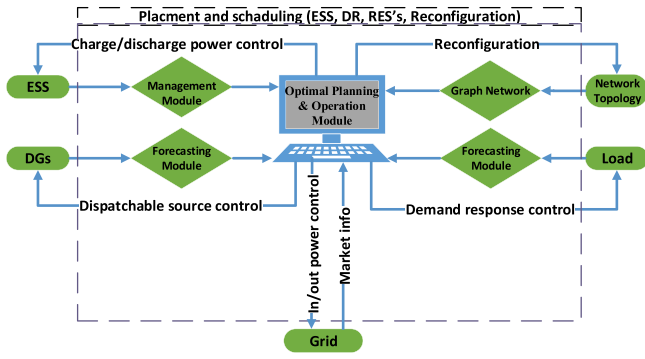


Fig. 1. Conceptual description of the proposed ORESA-DSR method.

2.2. Mathematical formulation of the proposed ORESA-DSR

The energy management problem in a typical DS is to allocate optimal power generation schedules as well as suitable allocation of ESSs and DR in such a way that both the power procurement cost of the DS and the reliability cost of the grid are minimized simultaneously, while satisfying several operational and physical constraints. The optimal power flow problem (OPF) is generally nonlinear program (NLP) optimization problem. When dealing with the placement of RESs, ESSs and DR, it becomes mixed-integer nonlinear (MINLP), which is generally hard to solve. Because of the non-convex nature of the AC OPF model, the conventional nonlinear optimization methods and meta-heuristic methods cannot guarantee the convergence of the solution methodology as well as global optimality. By applying some relaxations, it is possible to convert the NLP model of AC-OPF problem to a convex model. In this paper, by utilizing a proper relaxation technique, the NLP model AC-OPF model is relaxed to a second-order-cone programming (SOCP) model. Since the proposed ORESA-DSR model consists of placement variables which are inherently binary variables, a mixed-integer second-order-cone programming (MISOCP) model will be developed in the following. It has been shown that the MISOCP has better convergence and in the case of feasible search space, it converges the global optimal solution. The mathematical formulation of the proposed ORESA-DSR model based on the MISOCP is expressed as follows.

2.2.1. Objective functions

The DGs are optimally allocated in the DS by simultaneously minimizing two objective functions, in a multi-objective optimization model. These objective functions are described as follows.

Energy procurement cost: The DNO is responsible for energy procurement from the day-ahead electricity market. The day-ahead market mechanism is followed in many countries such as Ireland, Greece and Poland [32]. In this framework, the electricity prices are set based on market clearing mechanism one day in advance of actual operation of the system. The DNO is assumed to be price taker. However, in some regulatory frameworks like Nordic countries the real time and intra-day balancing market [33] is used. The energy procurement cost (EPC) of the system is expressed as follows.

$$EPC = \sum_{t \in \Omega_t} \sum_{i \in \Omega_n} \left[P_{i,t}^G + (P_{i,t}^{dch} - P_{i,t}^{ch}) + (P_{i,t}^D - P_{i,t}^{D0}) + P_{i,t}^W + P_{i,t}^0 \right] \times \kappa_t \quad (1)$$

where, κ_t is the electricity price of utility at time slot t . The EPC consists of the cost of energy purchase from the upstream network,

ESS, DR action, and RES at time t . It is obvious that the proper location and scheduling of the energy management options (i.e. RESs, ESS and DR) can decrease energy cost paid in the system.

Reliability index: distribution system as the last link between the production part and the consumers plays an important role to improve the reliability and power quality of the supply. In comparison with the generation and transmission networks, the distribution system is cheap and outages/failures of this part have a local impact on the consumers. Nevertheless, according to the failure statistics, the distribution systems have the most influence to the unavailability of supply to the consumers [31].

Energy not supplied (ENS) is one of the main system oriented reliability indices used for power systems. This index means the volume of energy that is lost as a result of faults or failures on the network. In this paper, cost of cost of ENS (CENS) is considered as an objective function, in addition to EPC. In DSs CENS is mainly related to the failure rate of branches. The DNO aims to reduce CENS as much as possible, since the interruption of customer loads, forces the DNO to pay value of lost load (VOLL) to the affected customers. CENS is defined as follows.

$$ENS = \sum_i FOR_i \times D_i \quad i \in \text{set of Failures} \quad (2)$$

$$FOR_i = \frac{\lambda_i \times U_i}{8760} \quad i \in \text{set of Failures} \quad (3)$$

where D_i is the total active power of load not supplied during failure i . Also, FOR , λ_i and U_i are respectively the forced outage rate, failure rate (in failure/year) and repair time (in hours) of a branch which leads to the i -th failure.

To be able to calculate this index in the proposed ORESA-DSR approach, it should be rewritten as a function of absolute power flowing through the branch, in time t .

$$ENS_t = \sum_{l \in \Omega_l} FOR_l |P_{l,t}| \quad (4)$$

where FOR_l is the FOR of the l -th branch. The most common way to linearize the above expression of ENS, is to use positive auxiliary variables. For example, suppose the absolute value of variable x is required. By defining positive variables x^+ and x^- , the constraints (5)–(10) yield the absolute value of variable x , as follows.

$$|x| = x^+ + x^- \quad (5)$$

$$x = x^+ - x^- \quad (6)$$

$$0 \leq x^+ \leq M \times z^+ \quad (7)$$

$$0 \leq x^- \leq M \times z^- \quad (8)$$

$$z^+ + z^- = 1 \quad (9)$$

$$z^+, z^- \in \{0, 1\} \quad (10)$$

where M in (7) and (8) is a sufficiently big positive constant (Big-M). Also, $z^{+/-}$ are binary variables. Hence, using the above linearization for $|P_{l,t}|$, the CENS could be expressed as follows.

$$CENS = \sum_{t \in \Omega_t} ENS_t \times VOLL_t \quad (11)$$

where $VOLL_t$ is the value of lost load at time t .

2.2.2. Problem constraints

2.2.2.1. Network reconfiguration constraints. The radial distribution network graph has a tree structure without any loops. The total number of lines equals the number of buses minus one [15]. Equation (12) guarantees that the tree structure for the DS.

$$\sum_{l \in \Omega_l} z_l^r = \Omega_n - 1 \quad (12)$$

2.2.2.2. Power flow equations. As it is aforementioned, in order to develop a convex optimization model for the proposed ORESA-DSR, LFB model is used to characterize AC power flow equations as follows [15].

$$\forall i \in \Omega_n, \forall t \in \Omega_t, \forall l \in \Omega_l : \sum_{l \in \Omega_l} A_{li} P_{l,t}^{net} = P_{i,t}^G + P_{i,t}^W + P_{i,t}^p - P_{i,t}^D - P_{i,t}^{ch} + P_{i,t}^{dch} - \sum_{l \in \Omega_l} B_{li} R_l J_{l,t} \quad (13)$$

$$\sum_{l \in \Omega_l} A_{li} Q_{l,t}^{net} = Q_{i,t}^G + Q_{i,t}^W - Q_{i,t}^D - \sum_{l \in \Omega_l} B_{li} X_l J_{l,t} - (1 - z_l^r) M \leq U_{j,t} - 2 \sum_{l \in \Omega_l} B_{lj} (R_l P_{l,t}^{net} + X_l Q_{l,t}^{net}) \quad (14)$$

$$-U_{i,t} + (R_l^2 + X_l^2) J_{l,t} \leq (1 - z_l^r) M \quad (15)$$

$$(P_{l,t}^{net})^2 + (Q_{l,t}^{net})^2 = J_{l,t} U_{i,t} \quad \forall A_{li} > 0 \quad (16)$$

$$(V^{\min})^2 \leq U_{i,t} \leq (V^{\max})^2 \quad (17)$$

$$0 \leq J_{l,t} \leq (I_l^{\max})^2 \quad (18)$$

where, $U_{i,t} = V_{i,t}^2$ & $J_{l,t} = I_{l,t}^2$.

Also, since only the connection to the upstream network is possible via the substation, the following constraint should be considered:

$$P_{i,t}^G = \begin{cases} P_t^{Ups} & i \in \Omega_s, \\ 0 & otherwise \end{cases} \quad (19)$$

$$Q_{i,t}^G = \begin{cases} Q_t^{Ups} & i \in \Omega_s, \\ 0 & otherwise \end{cases} \quad (20)$$

$P_{l,t}^{net}$, $Q_{l,t}^{net}$ in (2.2.2) and (14) are active/reactive power flow through line l at time t , respectively. Also, (2.2.2) describes the voltage transmit along the branch where the voltage drop on the line is quadratically related to the active/reactive power, voltage and line conductance. Equation (16) is nodal relationship between power, voltage and current. (17) and (18) describe the lower/upper bounds of quadratic bus voltage ($U_{i,t}$) and line current ($J_{l,t}$) at time t .

A_{li} is lj -th element of the bus-line incidence matrix, which is equal to 1, if bus i is the sending bus of line l , -1 if bus i is the receiving bus of line l , and 0 otherwise. Also, B_{li} is the modified A_{li} with all '+1' set to 0.

In this paper Big-M concept is employed to represent the network reconfiguration concept. When the line is open, $z_l^r = 0$, then equation (2.2.2) will be relaxed. If $z_l^r = 1$, then the voltage drop constraint must be satisfied.

Besides, $(P/Q)_{i,t}^G$ and $(P/Q)_{i,t}^W$ in (2.2.2) and (14) are the active and reactive power injected to the network by the upstream grid and WTs. It is obvious that $(P/Q)_{i,t}^G$ are only non-zero in the nodes connected to the upstream grid. Besides, $P_{i,t}^p$ is the power injected by PV cells. Ω_n, Ω_l are the set of system nodes and branches, respectively. $P_{i,t}^{ch}$, $P_{i,t}^{dch}$ are the charged/discharged power of ESS in (2.2.2).

It is observed that some of the power flow constraints are linearized or convexified, except (16), which is remained non-convex. To convexify this constraint, conic relaxation technique [34] is utilized to relax it to the following inequality constraint.

$$(P_{l,t}^{net})^2 + (Q_{l,t}^{net})^2 \leq J_{l,t} U_{i,t} \quad \forall A_{li} > 0 \quad (21)$$

Now, the above relaxed ORESA-DSR model is a special case of MISOCP problems. MISOCP optimization problems can be solved efficiently by high performance commercial solvers, such as CPLEX, GUROBI, MOSEK, etc. [35].

The sufficient conditions under which the above relaxation is exact have been exploited deeply in Refs. [36,37]. Roughly speaking, if the bus voltages is kept around the nominal value and the power injection at each bus is not too large, then the relaxation of (16) to (21) is exact, i.e. the global solution of the MISOCP-based ORESA-DSR is also a global optimal solution of the original non-convex ORESA-DSR model. In this paper, the sufficient conditions specified in Ref. [37] hold for the distribution grid and thus we focus on solving the MISOCP-based ORESA-DSR problem.

Finally, using the technique presented by ((5)–(10)) the absolute value of the active power flowing through a branch is obtained by (22) and (26):

$$\forall t \in \Omega_t ; \forall l \in \Omega_l \quad |P_{l,t}^{net}| = (P_{l,t}^{net})^+ + (P_{l,t}^{net})^- \quad (22)$$

$$P_{l,t}^{net} = (P_{l,t}^{net})^+ - (P_{l,t}^{net})^- \quad (23)$$

$$0 \leq (P_{l,t}^{net})^+ \leq M z_{t,l}^{to} \quad (24)$$

$$0 \leq (P_{l,t}^{net})^- \leq M z_{t,l}^{from} \quad (25)$$

$$z_{t,l}^{to} + z_{t,l}^{from} = z_l^r \quad (26)$$

Due to the non-linearity of constraint (4), it is linearized using constraints (22)–(26). $z_{t,l}^{to}$ and $z_{t,l}^{from}$ are binary variables which show the direction of power flow in the line l at time t . When the line l is open, i.e. $z_l^r = 0$, then the constraints (24) and (25) will be equal 0. When the line is closed, i.e. $z_l^r = 1$, then one of the constraints (24) or (25) will be non-zero and the absolute value of power flowing through line l could be determined by (22).

2.2.2.3. WT and PV constraints. The WT and PV scheduling constraints could be expressed as follow:

$$\forall i \in \Omega_n, \forall t \in \Omega_t, \forall l \in \Omega_l : \quad (27)$$

$$0 \leq P_{i,t}^w \leq \Phi_t^w \times \Lambda_i^w \times z_i^w$$

$$\chi_i^- \times P_{i,t}^w \leq Q_{i,t}^w \leq \chi_i^+ \times P_{i,t}^w \quad (28)$$

$$0 \leq P_{i,t}^p \leq \Phi_t^p \times \Lambda_i^p \times z_i^p \quad (29)$$

$$\sum_{i \in \Omega_n} z_i^w \leq MN^w \quad (30)$$

$$\sum_{i \in \Omega_n} z_i^p \leq MN^p \quad (31)$$

Equations (27) and (28) are the active and reactive power generation limits of the WT connected to bus i in time t , respectively. Also, (29) is the PV active power generation limit. z_i^w and z_i^p in (30) and (31) are the binary variables specify the presence (if equal 1) or absence (if equal 0) of WT and PV connected to bus i , respectively. Equations (30) and (31) models the maximum number of WTs and PVs that could be installed in the network.

2.2.2.4. ESS constraints. The ESS technical operating constraints to be satisfied ($\forall i \in \Omega_{ESS}, \forall t \in \Omega_t$) are as follows.

$$ES_{i,t} = ES_{i,t-1} + \left(\eta_{ch} P_{i,t}^{ch} - \frac{1}{\eta_{dch}} P_{i,t}^{dch} \right) \Delta t \quad (32)$$

$$ES_i^{\min} \leq ES_{i,t} \leq ES_i^{\max} \quad (33)$$

$$P_i^{ch,\min} z_i^{ESS} \leq P_{i,t}^{ch} \leq P_i^{ch,\max} z_i^{ESS} \quad (34)$$

$$P_i^{dch,\min} z_i^{ESS} \leq P_{i,t}^{dch} \leq P_i^{dch,\max} z_i^{ESS} \quad (35)$$

$$\sum_{i \in \Omega_n} z_i^{ESS} \leq MN^{ESS} \quad (36)$$

where Ω_{ESS} is the set of nodes which are equipped with ESS. The energy stored in a ESS in time t and bus i , $ES_{i,t}$, depends on its stored energy in time $t - 1$ and its charge and discharge states at time t (i.e. $P_{i,t}^{ch}, P_{i,t}^{dch}$). This relationship is described in (32). η_{ch} and η_{dch} are the charge and discharge efficiencies, respectively. The stored energy in ESS should be kept between specific limits ($ES_i^{\max/\min}$) as enforced by (33). The charge and discharge limits of ESS are given in (34) and (35), respectively. Also, (36) models the maximum number of ESSs that could be scheduled in the network.

2.2.2.5. DR constraints. Demand response constraints are expressed as follows ($\forall i \in \Omega_{DR}$ and $\forall t \in \Omega_t$).

$$P_{i,t}^D = P_{i,t}^{D0} \times \xi_{i,t} \quad (37)$$

$$Q_{i,t}^D = Q_{i,t}^{D0} \times \xi_{i,t} \quad (38)$$

$$\sum_{t \in \Omega_T} P_{i,t}^D = \sum_{t \in \Omega_T} P_{i,t}^{D0} \quad (39)$$

$$\sum_{t \in \Omega_T} Q_{i,t}^D = \sum_{t \in \Omega_T} Q_{i,t}^{D0} \quad (40)$$

$$\left(1 - \xi_i^{\min} z_i^{DR} \right) \leq \xi_{i,t} \leq \left(1 + \xi_i^{\max} z_i^{DR} \right) \quad (41)$$

$$\sum_{i \in \Omega_n} z_i^{DR} \leq MN^{DR} \quad (42)$$

The set of demands participating in DR program is represented by Ω_{DR} . $(P/Q)_{i,t}^{D0}$ and $(P/Q)_{i,t}^D$ in (37), (38) specify the initial/modified demand pattern without/with DR activation in (37), (38). $\xi_{i,t}$ denotes the decision variable for changing the demand pattern. Besides, (39) and (40) ensure the energy of load before and after DR program remains constant (i.e. DR is activated via load shifting mechanism). The constraint (41) models the flexibility degree of the demands. $\xi_i^{\max/\min}$ specify the maximum possible increase and decrease of demand in node i . z_i^{DR} is a binary variable; If $z_i^{DR} = 0$ then the node i does not participate in a DR program and contrarily, if $z_i^{DR} = 1$ it means bus i participates in the DR program. The total number of nodes which can participate in the DR program are limited by (42).

2.2.3. Decision variables

The decision variables (DV), parameters (U) and the sets are as follows:

$$DV = \left\{ U_{i,t}, J_{l,t}, (P/Q)_{i,t}^{G/D}, (P/Q)_{i,t}^w, P_{i,t}^p, ES_{i,t}, P_{i,t}^{ch}, P_{i,t}^{dch}, EPC, ENS_t, CENS, \xi_{i,t}, z_i^w, z_i^p, z_i^{ESS}, z_i^{DR}, z_l^r, z_{t,l}^{to}, z_{t,l}^{from} \right\} \quad (43)$$

$$U = \left\{ V^{\min/\max}, I^{\max}, R_l, X_l, (P/Q)_{i,t}^{D0}, \Phi_t^w, \Phi_t^p, \Lambda_i^w, \Lambda_i^p, ES_i^{\min/\max}, \eta_{ch/dch}, A_{li}, B_{li}, P_i^{ch,\min/\max}, P_i^{dch,\min/\max}, FOR_l, K_t, MN^{DR}, MN^{ESS}, MN^p, MN^w \right\} \quad (44)$$

$$Sets = \{ \Omega_{DR}, \Omega_t, \Omega_n, \Omega_l, \Omega_{ESS}, \Omega_w, \Omega_p \} \quad (45)$$

2.3. Multi-objective optimization problem

The proposed ORESA-DSR model is a multi-objective optimization problem, with the aim of optimizing two objective functions, namely EPC (given by (2.2.1)) and CENS ((11)), simultaneously subject to the aforementioned constraints. There are several methods to deal with multi-objective optimization problems. The most famous methods are the weighted sum approach and the ϵ -constraint method [38]. The ϵ -constraint method can return the solutions for both convex and non-convex Pareto optimal sets, while the weighted sum method is useable for convex Pareto sets only. In order to find the most satisfying solution from the non-dominated solution set, fuzzy satisfying criterion [28] is utilized in this paper.

2.4. Procedure for implementation of the proposed ORESA-DSR model

The proposed ORESA-DSR model for optimal allocation of RESs, ESSs, DRs and optimal DSR is constructed using the constraints (2)–(4) & (12)–(45) with the objective functions of (1) and (11). In

order to obtain the best results from the proposed multi-objective optimization model, ϵ -constraint method is used to attain Pareto optimal front. Also, fuzzy satisfying criterion is utilized to select the compromise optimal point from the obtained Pareto optimal set. The steps involved in order to implement the proposed ORESA-DSR model are described as follow.

Step 0: Input data and initialization.

- Generation forecast of RESs in day ahead market (equations (27) and (29)).
- Demand forecast of consumers in day ahead market (equations (13), (14), (37) and (38)).
- Energy price forecast in day ahead market (equation (1)).
- Maximum number of WTs, PVs, ESSs and DR participants (equations (30), (31), (36) and (42)).
- Up/down limits of nodal voltages (equation (17)) and branch flows (equation (18)).
- Initial network topology and branch data.

Step 1: Determination of the best/worst values of CENS and EPC.

- Minimization of EPC (i.e. determination of the minimum value of EPC and the worst value of CENS)
- Minimization of CENS (i.e. determination of the minimum value of CENS and the worst value of EPC)

Step 2: Achieving Pareto optimal front using ϵ -constraint method.

Step 3: Choose the best compromise solution of Pareto-optimal using the fuzzy satisfying criterion.

Step 4: Output results.

- Optimal values of EPC and CENS, and the Pareto optimal solutions.
- Optimal allocation and scheduling of DR participants, ESSs, WTs and PVs.
- Optimal radial configuration of the DS.
- Optimal power procurement from the upstream network.

3. Case study and numerical results

3.1. Studied system data

The main purpose of this paper is to investigate the role of RES, ESS, DR and DSR to enhance the reliability of DS as well as to minimize the energy procurement cost. The proposed ORESA-DSR model is implemented in GAMS [39] environment and solved by GUROBI [40] solver running on an Intel R XeonTM CPU E5-1620 3.6 GHz PC with 8 GB RAM.

In this regard, some assumptions are made to evaluate the reliability indices. About the failure rate, it is supposed that the line with the highest impedance has the failure rate of 0.4 f/yr and the line with the least impedance has the failure rate of 0.1 f/yr. Consequently, the failure rate of other lines can be evaluated according to these two values, proportionally. The repair time is assumed to be 2 h [2]. Also, the VOLL is assumed to be 20 \$/kWh [7]. The proposed model is applied on the IEEE standard 33-bus DS [10]. The single line diagram of this system is depicted in Fig. 2. The upper and lower voltage limits on the nodes are 1.10 pu. and 0.90 pu., respectively. As well as the current limit on all feeders is 0.06 pu. The peak demand value used in this study is higher than what is reported in Ref. [10] in order to make a heavy loaded DS. The considered peak load of the system is 4.643 MW. The load demand of this system, along with the WT and PV forecasted hourly

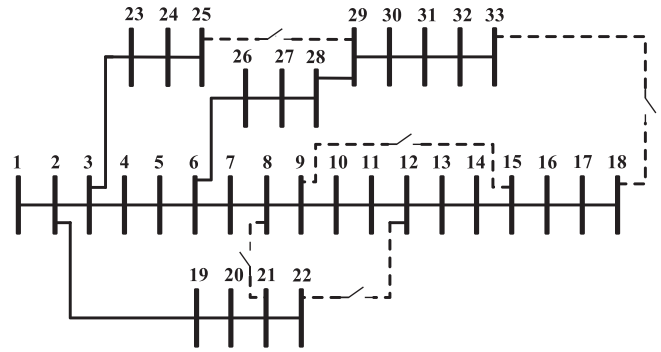


Fig. 2. Single-line diagram of the IEEE 33-node DS.

power outputs are given in Table 2 for a typical 24 h time period. The forecasted power outputs of WT and PV adopted from Refs. [22,30], respectively. It is worth to note that these values for demand, WT and PV power generations are respected to the corresponding peak values; for example, in time slot 18, the total load of the system is $1.000 \times 4.643 MW = 4.643 MW$. The energy market prices for the considered period are given in Table 2 [29]. As it is also shown in Fig. 2, there are 32 normally closed lines and 5 normally open lines in the studied system. The optimal radial structure of the system could be determined via the proposed ORESA-DSR model.

Also, the rated capacity of each WT, PV and capacity of ESS is assumed to be 0.50 MW. The coefficients for modeling lower/upper limits of WT reactive power outputs (i.e. $\chi_i^{-/+}$) are -0.80 and $+0.80$, respectively. The technical characteristics of the considered ESS are described in Table 3. Without loss of generality, it is supposed that the DNO aims to optimally allocate two WTs, PVs, ESSs and DR participants (i.e. $MN^{ESS} = MN^{DR} = MN^w = MN^p = 2$) in the network for the given load and energy price. The flexibility degree can be adjusted by changing the $\xi_{i,t}^{min/max}$ in (41). It is also assumed that $\xi_{i,t}^{min/max} = 0.5$.

Table 2
Forecasted hourly demand, output power of WTs & PVs, energy price.

h	Demand [6]	Φ_t^w [30]	Φ_t^p [22]	energy price [29]
1	0.719	0.815	0	28.0
2	0.674	0.880	0	24.0
3	0.624	0.886	0	22.0
4	0.588	0.880	0	22.5
5	0.582	0.881	0	23.5
6	0.588	0.881	0	25.0
7	0.600	0.953	0	27.5
8	0.633	0.987	0.008	31.5
9	0.644	0.985	0.050	37.5
10	0.730	0.962	0.125	44.0
11	0.793	1.000	0.418	42.5
12	0.844	0.979	0.511	40.0
13	0.875	0.945	0.516	42.0
14	0.868	0.776	0.475	43.0
15	0.851	0.673	0.418	46.0
16	0.875	0.591	0.254	47.5
17	0.951	0.487	0.050	48.5
18	1.000	0.466	0	48.5
19	0.981	0.373	0	50.0
20	0.948	0.339	0	44.5
21	0.900	0.339	0	38.0
22	0.875	0.372	0	36.0
23	0.801	0.393	0	30.0
24	0.722	0.339	0	26.0

Table 3
The technical characteristics of ESS.

Parameter	Value	Unit
$ES_{i,t}^{max}$	0.5(500 KWh REDOX batteries [27])	MWh
$ES_{i,t}^{min}$	0	MWh
$p_{i,t}^{ch,max} = p_{i,t}^{dch,max}$	0.100	MW
$p_{i,t}^{ch,min} = p_{i,t}^{dch,min}$	0	MW
$\eta_{ch} = \eta_{dch}$	95	%

3.2. Considered cases

In this paper four different cases are studied as follows.

Case I:

The network is studied in the base case condition. This case is added for the purpose of providing a basis for comparison, and neither WTs, PVs, ESSs, DRs and nor DSR is considered. No optimization is performed in this case and just a basic power flow problem is solved. Hence, the constraints to be satisfied are (2.2.2)–(21). The decision variables of this case are limited to load flow variables as follows. $DV_1 = \{U_{i,t}, J_{i,t}, P_{i,t}^G, Q_{i,t}^G\}$.

Case II:

CENS minimization (i.e. the objective function is (11)). The minimum value of CENS is attained by considering optimal placement and scheduling of WTs, PVs, ESSs and DRs, along with the DSR. The constraints to be satisfied are (12)–(42). This implies that:

$$DV_2 = DV_1 \cup \left\{ \begin{matrix} (P/Q)_{i,t}^w, p_{i,t}^p, ES_{i,t}, p_{i,t}^{ch}, p_{i,t}^{dch}, \\ \xi_{i,t}, ENS_t, CENS, z_i^w, z_i^p, z_i^{ESS}, z_i^{DR}, \\ z_1^r, z_{t,l}^{to}, z_{t,l}^{from} \end{matrix} \right\} \quad (46)$$

Case III:

In this case the best compromise solution is obtained by simultaneously consideration of CENS and EPC via a multi-objective optimization model. The Pareto optimal solutions are obtained by ϵ -constraint method and the best compromise solution is selected by fuzzy satisfying criterion. The constraints to be satisfied are (12)–(42). The set of decision variables in this case are those given in (43), i.e. $DV_3 = DV$.

Case IV:

EPC minimization (i.e. the objective function is (2.2.1)). The constraints to be satisfied are (12)–(42). The decision variables in this case are as follows.

$$DV_4 = DV_1 \cup \left\{ \begin{matrix} (P/Q)_{i,t}^w, p_{i,t}^p, ES_{i,t}, p_{i,t}^{ch}, p_{i,t}^{dch}, \\ \xi_{i,t}, EPC, z_i^w, z_i^p, z_i^{ESS}, z_i^{DR}, \\ z_1^r, z_{t,l}^{to}, z_{t,l}^{from} \end{matrix} \right\} \quad (47)$$

3.3. Results

The optimal results obtained for the aforementioned cases are

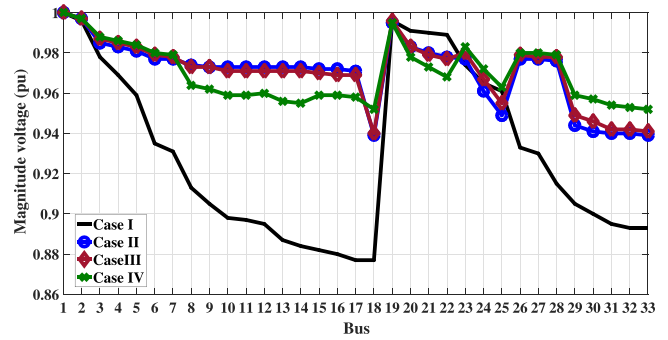


Fig. 3. Voltage profile of the system at the peak load (i.e. hour 18).

presented and discussed in the following. For the sake of brevity and comparison, the results of all cases are presented together in some figures and tables.

Case I:

In this case, the CENS is \$ 497.49 and EPC is \$ 3448.70. Fig. 3 shows the voltage profile of the system in the peak loading condition (i.e. the hour 18). As shown in this figure, in Case I the bus voltages vary from 0.877 pu to 1.000 pu.

Case II:

In this case the aim is to minimize the CENS. The optimal value of CENS is \$ 268.58, which shows a 46.01% reduction in comparison with Case I. Also, in this case, the EPC is \$ 3298.64, which means a 4.35% reduction with respect to Case I. The optimal locations of WTs, PVs, ESSs and DR in all cases (i.e. Case I–Case IV) are given in Table 4. In this table, for each case, the values of EPC and CENS are presented. Furthermore, the optimal reconfiguration of network (i.e. the open circuited lines) and the percentages of reduction in CENS and EPC are given for all cases, in order to simplify the comparison between these cases.

As can be seen from Table 4, optimal locations the ESSs and PVs are nodes 17 and 18 in Case II. The state of charge, charge and discharge patterns of ESSs are depicted in Fig. 4. It is worth to mention that the ESSs are charged when the PVs inject power to the grid (i.e. at hours 8–15 for the ESS located in bus 17, and during the hours 7–15 for the ESS connected to node 18). But, the discharge action is activated in the peak loading conditions, i.e. during the hours 17–24 for the ESS located at bus 17 and the hours 17–22 for the ESS of node 18.

In this case the buses 14 and 32 are determined as the optimal nodes for DR provision. The new demand pattern of these buses are

Table 4
Comparison of results in the different cases.

CASE	I	II	III	IV
CENS(\$)	497.49	268.58	275.01	292.25
EPC(\$)	3448.70	3298.64	3187.88	3160.18
WTs locations	–	14, 32	14, 32	30, 32
PVs locations	–	17, 18	17, 30	14, 17
ESSs locations	–	17, 18	14, 17	17, 32
DRs locations	–	14, 32	24, 25	24, 25
Open lines	8-21, 9-15	7-8, 9-10,	7-8, 9-10	7-8, 9-10
	12-22, 18-33	17-18, 9-15	17-18, 9-15	17-18, 14-15
	25-29	28-29	28-29	28-29
CENS reduction (%)	–	46.01	44.71	41.25
EPC reduction (%)	–	4.35	7.56	8.36

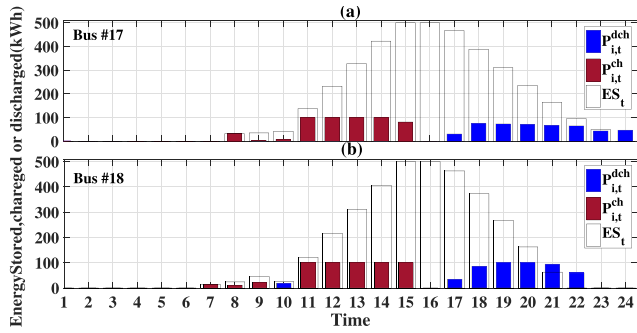


Fig. 4. The hourly energy stored, charge/discharge patterns of ESSs in Case II: (a) node #17, (b) node #18.

depicted in Fig. 5(a). The load shifting via DR program in these buses is done by considering the energy price and load demand for the entire horizon, such that in the modified load curve, the load is shifted from the peak hours to the off-peak hours. Also, the optimal places for WTs are nodes 14 and 32. Due to the high available generation of the WTs in the hours 1–14, DR program increases the demand of nodes 14 and 32 in these hours. For the remaining hours, the demand is reduced.

Besides, in this case the optimal generation schedule of RESs along with the power purchased from the upstream network, are given in Table 5. The voltage profile of the system in the peak loading condition (i.e. the hour 18), is also depicted in Fig. 3. It is evidently observed from this figure that, by optimal allocation of energy generation/management facilities such as RESs, DR, ESS and DSR, the voltage profile of the system is improved considerably.

Case III:

In this case, the EPC and CENS are minimized via a multi-objective optimization model. The optimal radial configuration of the DS as well as the optimal allocation of WTs, PVs, ESSs and DRs are depicted in Fig. 6 at this case. The proposed multi-objective ORESA-DSR model is solved via ϵ -constraint method. According to Fig. 7, the EPC and CENS are conflicting objectives, such that reduction of one objective function results in deterioration of the other objective. In such non-dominated Pareto optimal solutions, the decision maker (here the DNO) aims to find a compromise solution which yields a proper balance between the EPC and CENS. In this paper, the compromise solution is obtained by fuzzy satisfying criterion. This solution is also shown in Fig. 7.

As shown in Fig. 7 at the best compromise solution, the EPC and CENS are \$ 3187.88 and \$ 275.01, respectively. By referring to

Table 5
Optimal power dispatch in Case II.

Time(h)	$P_{i,t}^w$ (kW)		$P_{i,t}^p$ (kW)		$P_{i,t}^e$ (kW)
	Bus #14	Bus #32	Bus #17	Bus #18	
1	407.500	407.500	0	0	2675.999
2	440	440	0	0	2438.501
3	443	443	0	0	2179.820
4	440	440	0	0	2005.059
5	440.500	440.500	0	0	1973.930
6	440.500	440.500	0	0	2004.014
7	476.500	476.500	0	0	2005.347
8	493.500	493.500	4	4	2157.308
9	492.500	492.500	25	25	2152.676
10	481	481	62.500	62.500	2496.316
11	500	500	209	209	2691.325
12	489.500	489.500	228.547	255.500	2904.594
13	472.500	472.500	258	258	3042.475
14	388	388	237.500	237.500	3068.485
15	336.500	336.500	209	209	3020.985
16	295.500	295.500	127	127	3124.156
17	243.500	243.500	25	25	3740.778
18	233	233	0	0	3949.713
19	186.500	186.500	0	0	3947.246
20	169.500	169.500	0	0	3829.410
21	169.500	169.500	0	0	3609.999
22	186	186	0	0	3494.825
23	196.500	196.500	0	0	3208.651
24	169.500	169.500	0	0	2892.015

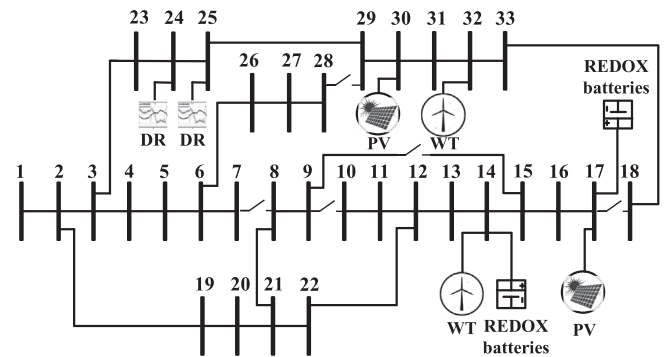


Fig. 6. Optimal configuration of the system along with optimal allocation of WTs, PVs, ESSs and DRs in Case III.

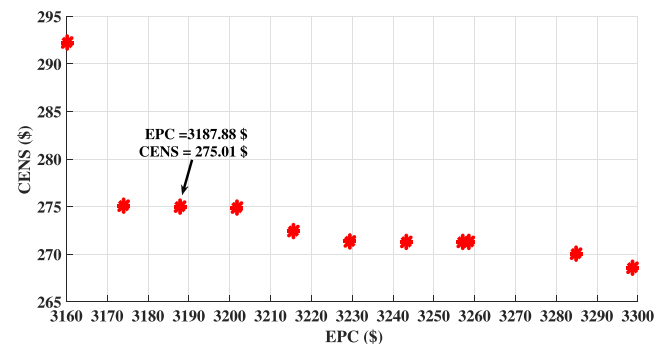


Fig. 7. Pareto optimal front of EPC versus CENS.

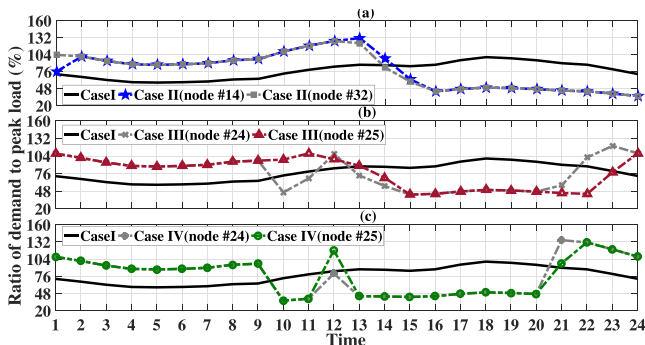


Fig. 5. The hourly demand pattern in different cases (comparison with Case I): (a) Case II, (b) Case III, (c) Case IV.

Table 4, this strategy can reduce the EPC and CENS up to 7.56% and 44.71%, respectively in comparison with Case I. The optimal placement of WTs, PVs, ESSs and DRs in this case is also given in Table 4. In this case the optimal locations for DR activation are buses #24 and #25. The new demand patterns of these buses, are

depicted in Fig. 5(b). Similar to Case II, this new pattern is determined by considering the optimal locations of ESSs, WTs and PVs, as well as the hourly electricity price. It is evidently observed from the Fig. 5(b) that since the energy price at hours 1–9 and 22–24 is relatively low, the demand is shifted to these hours. In addition, due to the high energy price at hours 14–20, the load demand reduced in these hours. Also, the demand of node 24 is more sensitive to the energy price variations, such that in hour 10 by sudden increase of energy price, the demand of this bus reduced considerably. Also, according to Fig. 3, in this case the voltage profile is also improved considerably compared to the base-case (i.e. Case I).

As can be seen from Table 4, in this case the optimal locations for ESSs are the nodes #14 and #17. The state of charge along with charging/discharging patterns of ESSs are depicted in Fig. 8. It is worth to note that the charging process of the ESSs is done at the hours of the day when the available power generation of RESs is high, but the discharge action is postponed to peak loading hours. The optimal power dispatch in Case III is presented in Table 6.

Case IV:

In this case, the aim is to minimize the EPC. For this case, the

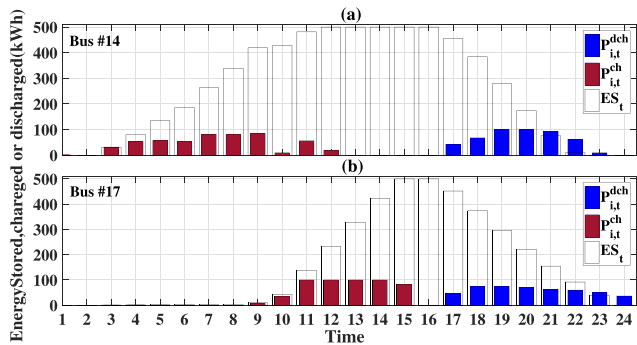


Fig. 8. The hourly energy stored and charge/discharge patterns of ESSs in Case III: (a) node #14, (b) node #17.

Table 6
Optimal power dispatch in Case III.

Time(h)	$P_{i,t}^w$ (kw)		$P_{i,t}^p$ (kw)		$P_{i,t}^c$ (kW)
	Bus #14	Bus #32	Bus #17	Bus #30	Bus #1
1	407.500	407.500	0	0	2980.227
2	440	440	0	0	2666.709
3	443	443	0	0	2422.733
4	440	440	0	0	2256.177
5	440.500	440.500	0	0	2227.388
6	440.500	440.500	0	0	2255.637
7	476.500	476.500	0	0	2273.739
8	493.500	493.500	4	4	2406.367
9	492.500	492.500	25	25	2435.374
10	481	481	62.500	62.500	2389.195
11	500	500	208.995	209	2574.499
12	489.499	489.500	226.638	255.500	2844.032
13	472.500	472.500	231.294	258	2725.562
14	388	388	237.500	237.500	2692.561
15	336.500	336.500	209	209	2551.372
16	295.500	295.500	127	127	2828.254
17	243.500	243.500	25	25	3394.382
18	233	233	0	0	3629.998
19	186.500	186.500	0	0	3615.514
20	169.500	169.500	0	0	3509.652
21	169.500	169.500	0	0	3382.755
22	186	186	0	0	3524.391
23	196.500	196.500	0	0	3581.316
24	169.500	169.500	0	0	3470.518

optimal DSR and locations for WTs, PVs, ESSs and DRs are presented in Table 4. As a result of DR program, the new demand patterns of buses #24 and #25 are depicted in Fig. 5(c) for this case. Given that in this case, the goal is to minimize the EPC, performance of DR program is mainly influenced by the cost of energy over the entire horizon. It can be seen from Fig. 5(c), that more load than the previous cases is shifted to the off-peak intervals (i.e. the hours 1–9 and 22–24). Also, since at the hour 12, the energy price is suddenly decreased, the DR acts to increase the demand in this hour. As shown in Table 4, the EPC is \$ 3160.18, whereas the CENS is \$ 292.25. Hence the EPC and CENS are decreased 8.36% and 41.25% in comparison with Case I. Also, in this case the optimal locations of ESSs are the nodes #17 and #32. The optimal schedule of ESSs is depicted in Fig. 9. As it is observed from this figure, the ESS located in node #32, will be charged to its maximum capacity at hour 10, and it is discharged in the peak loading condition to cope with the energy demand of the network.

For this case, the optimal energy share of different sources are presented in Table 7. Also, according to Fig. 3, the voltage profile in this case is also improved considerably compared to the Case I.

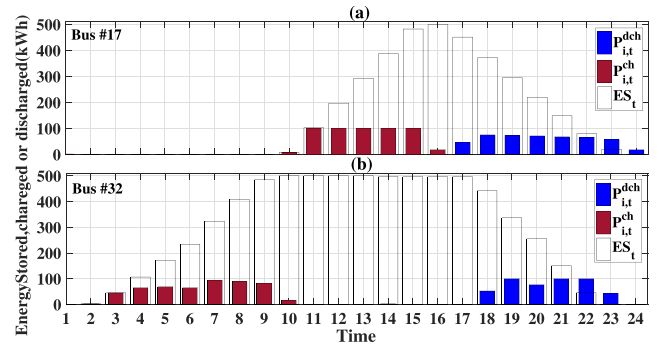


Fig. 9. The hourly energy stored, charge/discharge patterns of ESSs in Case IV: (a) node #17, (b) node #32.

Table 7
Optimal power dispatch in Case IV.

Time(h)	$P_{i,t}^w$ (kw)		$P_{i,t}^p$ (kw)		$P_{i,t}^c$ (kW)
	Bus #30	Bus #32	Bus #14	Bus #17	Bus #1
1	407.500	407.500	0	0	2963.844
2	440	440	0	0	2654.832
3	443	443	0	0	2423.898
4	440	440	0	0	2258.137
5	440.500	440.500	0	0	2229.518
6	440.500	440.500	0	0	2257.615
7	476.500	476.500	0	0	2276.151
8	493.500	493.500	4	4	2404.694
9	492.500	492.500	25	25	2413.648
10	481	481	62.500	62.500	1971.032
11	500	500	209	209	1975.708
12	489.500	489.500	255.500	255.5	2740.542
13	472.500	472.500	258	258	2279.416
14	388	388	237.500	237.500	2465.68
15	336.500	336.500	209	209	2563.332
16	295.500	295.500	127	127	2839.854
17	243.500	243.500	25	25	3429.603
18	233	233	0	0	3635.24
19	186.500	186.500	0	0	3605.162
20	169.500	169.500	0	0	3524.423
21	169.500	169.500	0	0	4092.058
22	186	186	0	0	4134.892
23	196.500	196.500	0	0	3768.485
24	169.500	169.500	0	0	3478.966

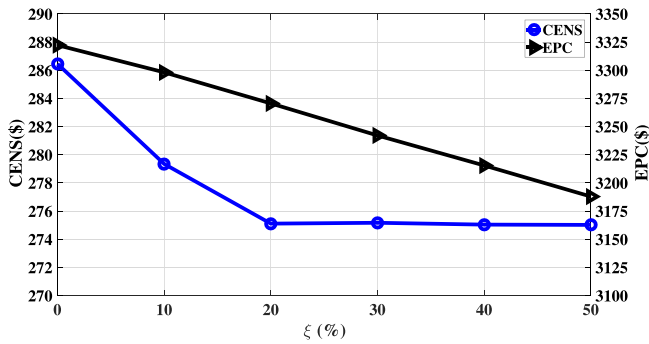


Fig. 10. Variation of EPC(\$)¹ and CENS(\$)² versus ξ (%).

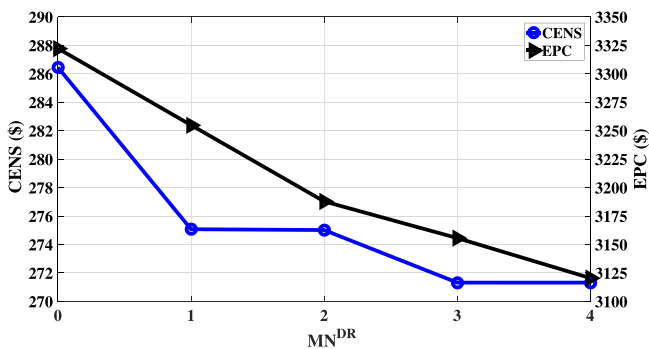


Fig. 11. Variation of EPC(\$)¹ and CENS(\$)² versus MN^{DR} .

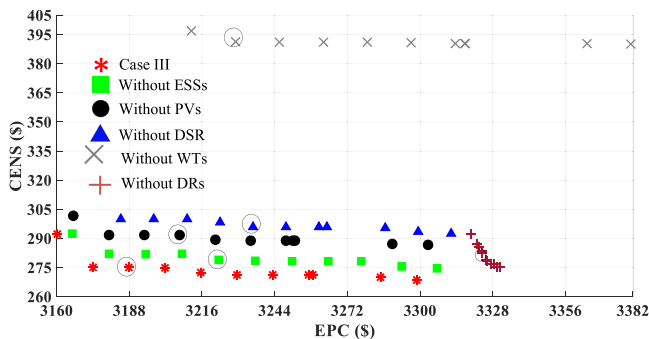


Fig. 12. The impact of various energy procurement/management tools on the CENS and EPC.

3.4. Sensitivity analysis

3.4.1. Sensitivity analysis on the DR participation

In order to evaluate the impact of participation rate (i.e. $\xi_{i,t}^{min/max}$) and number of DR participants (i.e. MN^{DR}) on the results, two sensitivity analysis are performed here. In the first analysis, the participation rate of DR is increased from 0% to 50% for the two customer participating in DR program (i.e. for $MN^{DR} = 2$), and its impact on EPC and CENS is investigated. The obtained results are depicted in Fig. 10. It is observed from this figure that by increasing the participation rate of DR from 0% to 20%, the CENS decreases from \$ 286.44 to \$ 275.10. By further increase of DR participation rate, the decrease of CENS is negligible such that it will be \$ 275.01 for the DR participation rate of 50%. Besides, by the increase of DR participation rate from 0% to 50%, the EPC decreases monotonically from \$ 3322.23 to \$ 3187.88, which shows the capability of DR for reduction of EPC.

Also, the impact of DR participant numbers is evaluated. Fig. 11 shows the impact of the number customers participating in DR program on EPC and CENS. It is observed from this figure that by increasing the DR participants from $MN^{DR} = 0$ to $MN^{DR} = 4$, the CENS decreases from \$ 286.44 to \$ 271.32. Besides, the EPC decreases monotonically from \$ 3322.23 to \$ 3120.48. This analysis substantiates the capability of DR program for reduction of both EPC and CENS.

3.4.2. Sensitivity analysis to evaluate the impact of WT, DR, PV, ESS and DSR on the Pareto optimal solution

In this case, the impact of each energy procurement/management tool (i.e. WTs, PVs, ESSs, DRs and DSR) on the Pareto optimal solution is investigated. The obtained Pareto fronts for different cases is illustrated in Fig. 12. Also, Table 8 summarizes the compromise solutions of different cases. It is observed from Fig. 12 and Table 8 that in presence of all energy procurement/management tools (i.e. Case III), the Pareto optimal front will be better than the other cases (i.e. both EPC and CENS are lower than the corresponding values in other states). Using the fuzzy satisfying criterion, the best compromise solutions are determined for all states, which are marked on each Pareto optimal front in Fig. 12.

It is also observed from Fig. 12 that the Pareto optimal front is affected considerably from the presence of WTs, such that in the case of WTs absence (i.e. without WTs), the CENS is almost the same for all Pareto optimal solutions. In the case of without WTs, the CENS and EPC are \$ 391.23 and \$ 3228.92, respectively. It is reduced 21.35% and 6.37% in comparison with Case I. However, The absence of WTs has the highest impact on the CENS compared to other cases, such that the CENS increased by 23.36% with respect to Case III.

Also, the absence of DR program has the highest impact on the

Table 8 Comparison of the best compromise solutions when excluding different energy procurement/management.

CASE	Case I	Case III	without DSR	without PV	without ESS	without WT	without DR
CENS(\$)	497.49	275.01	295.98	291.74	278.95	391.23	282.29
EPC(\$)	3448.70	3187.88	3235.63	3207.43	3222.45	3228.92	3323.85
WTs Locations	–	14, 32	15, 32	17, 31	15, 32	–	17, 32
PVs Locations	–	17, 30	18, 30	–	10, 31	18, 33	14, 30
ESSs Locations	–	14, 17	15, 18	18, 32	–	18, 33	17, 18
DRs Locations	–	24, 25	24, 32	24, 25	25, 32	24, 25	–
Open lines	8-21, 9-15 12-22, 18-33	7-8, 9-10 17-18, 28-29	8-21, 9-15 12-22, 18-33	7-8, 9-10 12-13, 28-29	7-8, 9-10 17-18, 28-29	7-8, 9-10 9-15, 17-18	7-8, 9-10 14-15, 17-18
	25–29	15–9	25–29	15–9	15–9	28–29	28–29
CENS reduction (%)	–	44.71	41.30	41.35	43.92	21.35	43.25
EPC reduction (%)	–	7.56	6.17	6.99	6.56	6.37	3.62

EPC, as depicted in Fig. 12 as shown in Table 8, without DR program, the EPC is \$ 3323.85 which is 3.62% lower than Case I. This value of EPC is 3.94% higher than Case III where all energy procurement/management are utilized.

3.5. The exactness of the utilized SOCP relaxation

In the proposed ORESA-DSR model, if the equality constraint (16) is relaxed to the inequality constraint (21), the problem will be a MISOCP optimization problem. If at the attained optimal solution of this relaxed optimization model, the equality constraint (16) satisfied, then this solution is also an optimal solution for the original non-convex ORESA-DSR model. In order to demonstrate the exactness of the relaxation, the numerical evaluation of each side of equation (21), as well as the difference between them, which should be less than or equal to zero, is given in Table 9. The given values corresponds to Case IV and the hour 18. It is observed from this table that the difference between two sides of (21) is very small and close to zero. In other words, although (21) is the relaxed form of the original equation (16), but this solution is also an optimal solution to the original non-convex ORESA-DSR model. A similar discussion exists for the remaining cases and the entire horizon. For example, the exactness of (21) for the most heavy loaded line, i.e. line 1 – 2 in different cases, is given in Table 10. The values given in this table, are the difference between two sides of (21) for this line. It is observed from this table that the employed relaxation, yields an exact optimal solution of the original non-convex model.

Table 9
Exactness checking of SOCP relaxation for Case IV at hour 18.

Sending Bus	Receiving Bus	Branch Number	$a = (P_{it}^{net})^2 + (Q_{it}^{net})^2$	$b = J_{lit}U_{it}$	$a - b$
1	2	1	7.05E-03	7.05E-03	-9.02E-17
2	3	2	3.05E-03	3.05E-03	-1.99E-17
2	19	18	9.72E-04	9.72E-04	-2.64E-17
3	4	3	3.01E-04	3.01E-04	-9.40E-15
3	23	22	1.05E-03	1.05E-03	7.00E-17
4	5	4	1.89E-04	1.89E-04	-1.36E-17
5	6	5	1.45E-04	1.45E-04	-7.82E-16
6	7	6	3.13E-05	3.13E-05	-7.50E-17
6	26	25	2.34E-05	2.34E-05	-1.50E-17
8	9	8	2.35E-05	2.35E-05	-8.80E-17
8	21	33	1.09E-04	1.09E-04	-2.00E-17
9	15	34	1.06E-05	1.06E-05	-8.90E-17
10	11	10	2.50E-06	2.50E-06	-1.63E-17
11	12	11	8.47E-06	8.47E-06	-1.52E-17
12	13	12	2.88E-05	2.88E-05	-1.39E-17
12	22	35	9.99E-05	9.99E-05	-1.42E-17
13	14	13	1.30E-05	1.30E-05	-7.43E-17
15	16	15	3.26E-06	3.26E-06	-6.41E-16
16	17	16	2.50E-07	2.50E-07	-1.44E-16
18	33	36	6.06E-06	6.06E-06	-7.43E-17
19	20	19	8.20E-04	8.20E-04	-1.53E-17
20	21	20	6.59E-04	6.59E-04	-1.65E-17
21	22	21	1.59E-04	1.59E-04	-1.52E-16
23	24	23	9.01E-04	9.01E-04	-2.31E-17
24	25	24	5.88E-04	5.88E-04	-2.17E-16
25	29	37	3.55E-04	3.55E-04	-6.08E-16
26	27	26	1.03E-05	1.03E-05	-1.86E-16
27	28	27	2.50E-06	2.50E-06	-1.51E-17
29	30	29	2.47E-04	2.47E-04	-6.19E-17
30	31	30	5.64E-05	5.64E-05	-1.34E-17
31	32	31	1.15E-05	1.15E-05	-1.42E-16
32	33	32	1.81E-05	1.81E-05	-8.15E-17
7	8	7	0.000	0.000	0.000
9	10	9	0.000	0.000	0.000
14	15	14	0.000	0.000	0.000
17	18	17	0.000	0.000	0.000
28	29	28	0.000	0.000	0.000

Table 10
Exactness checking of SOCP relaxation for different cases at bus 1 and line 1-2.

Time	Case I	Case II	Case III	Case IV
1	-6.80E-17	-3.60E-17	-8.64E-17	-2.38E-17
2	-1.73E-17	-3.57E-17	-2.29E-17	-6.64E-17
3	-4.56E-17	-1.43E-17	-4.70E-17	-3.93E-17
4	-7.47E-17	-1.87E-18	-4.14E-17	-7.52E-17
5	-7.22E-17	-8.99E-17	-5.79E-17	-7.34E-17
6	-5.25E-17	-4.40E-17	-6.72E-17	-8.69E-17
7	-3.18E-17	-1.35E-17	-5.58E-17	-6.53E-17
8	-5.67E-17	-3.13E-17	-5.15E-17	-4.62E-17
9	-6.24E-17	-8.95E-17	-3.69E-17	-3.60E-17
10	-8.71E-17	-2.48E-18	-6.74E-17	-4.07E-17
11	-6.57E-17	-6.42E-17	-2.12E-17	-2.02E-17
12	-8.63E-17	-5.10E-17	-6.44E-17	-5.39E-17
13	-1.23E-17	-4.23E-17	-1.96E-17	-6.98E-17
14	-8.43E-17	-6.89E-17	-1.24E-17	-4.98E-17
15	-6.80E-17	-7.66E-17	-6.19E-17	-8.22E-17
16	-2.64E-17	-4.83E-17	-1.45E-17	-1.25E-17
17	-6.87E-18	-4.78E-17	-5.34E-17	-8.80E-17
18	-3.11E-17	-4.04E-17	-8.45E-17	-9.02E-17
19	-6.94E-17	-5.56E-17	-6.39E-18	-6.89E-17
20	-8.23E-17	-2.48E-17	-1.61E-17	-5.66E-17
21	-1.68E-17	-8.52E-18	-7.30E-17	-8.53E-17
22	-4.12E-17	-4.27E-17	-2.35E-19	-1.36E-17
23	-5.46E-18	-1.97E-17	-4.09E-18	-1.62E-17
24	-8.61E-17	-7.94E-17	-3.45E-17	-1.52E-17

4. Conclusion

In this paper, a methodology is developed to find optimal reconfiguration of DSs and optimal allocation of RES, ESS and DR. The developed ORESA-DSR model is mathematically formulated as a MISOCP problem, which is convex and returns a global optimal solution. The proposed ORESA-DSR is a multi-objective optimization model with the objectives of EPC and CENS. ϵ -constraint technique is used to deal with these conflicting objectives and to attain the Pareto optimal solutions. Also, fuzzy satisfying criterion is utilized to select the best compromise solution. The benefits of the proposed model in terms of system economics and reliability are demonstrated through comparative case studies on the IEEE 33-bus standard DS. The DSR, RES, ESS and DR are used as energy generation/management options which enable the DNO to operate the system more efficiently.

Some of the main findings of this paper are summarized as follows:

- The EPC and CENS are decreased when the DR participation increases. This means the DR program is capable for reduction of power procurement cost.
- Among the energy procurement options, namely WTs and PVs, the impact of WTs in reduction of CENS is more considerable than PVs.
- Among the energy management options, namely DR, DSR and ESS, the impact of DR in reduction of EPC is more considerable than ESS and DSR.
- The convex SOCP-based relaxation of the proposed ORESA-DSR is exact and converges to the global optimal solution of the original non-convex ORESA-DSR optimization model.

References

[1] R.N. Allan, et al., Reliability evaluation of power systems, Springer Science & Business Media, 2013.
 [2] N.G. Paterakis, A. Mazza, S.F. Santos, O. Erdinc, G. Chicco, A.G. Bakirtzis, J.P. Catalão, Multi-objective reconfiguration of radial distribution systems using reliability indices, IEEE Trans. Power Syst. 31 (2) (2016) 1048–1062.
 [3] B. Amanulla, S. Chakrabarti, S. Singh, Reconfiguration of power distribution systems considering reliability and power loss, IEEE Trans. Power Deliv. 27 (2)

- (2012) 918–926.
- [4] A. Kavousi-Fard, T. Niknam, Optimal distribution feeder reconfiguration for reliability improvement considering uncertainty, *IEEE Trans. Power Deliv.* 29 (3) (2014) 1344–1353.
 - [5] A.A. Moghaddam, A. Seifi, T. Niknam, M.R.A. Pahlavani, Multi-objective operation management of a renewable mg (micro-grid) with back-up micro-turbine/fuel cell/battery hybrid power source, *Energy* 36 (11) (2011) 6490–6507.
 - [6] A. Soroudi, P. Siano, A. Keane, Optimal dr and ess scheduling for distribution losses payments minimization under electricity price uncertainty, *IEEE Trans. Smart Grid* 7 (1) (2016) 261–272.
 - [7] A. Ameli, S. Bahrami, F. Khazaeli, M.-R. Haghifam, A multiobjective particle swarm optimization for sizing and placement of dgs from dg owner's and distribution company's viewpoints, *IEEE Trans. Power Deliv.* 29 (4) (2014) 1831–1840.
 - [8] M.E. Soberanis, T. Mithrushi, A. Bassam, W. Mérida, A sensitivity analysis to determine technical and economic feasibility of energy storage systems implementation: A flow battery case study, *Renew. Energy* 115 (2018) 547–557.
 - [9] R. Al Abri, E.F. El-Saadany, Y.M. Atwa, Optimal placement and sizing method to improve the voltage stability margin in a distribution system using distributed generation, *IEEE Trans. Power Syst.* 28 (1) (2013) 326–334.
 - [10] M.E. Baran, F.F. Wu, Network reconfiguration in distribution systems for loss reduction and load balancing, *IEEE Trans. Power Deliv.* 4 (2) (1989) 1401–1407.
 - [11] P. Prasad, S. Sivanagaraju, N. Sreenivasulu, Network reconfiguration for load balancing in radial distribution systems using genetic algorithm, *Electr. Power Compon. Syst.* 36 (1) (2007) 63–72.
 - [12] M. Rider, A. Garcia, R. Romero, Power system transmission network expansion planning using ac model, *IET generation, Transm. Distrib.* 1 (5) (2007) 731–742.
 - [13] Y. Chen, A. Casto, F. Wang, Q. Wang, X. Wang, J. Wan, Improving large scale day-ahead security constrained unit commitment performance, *IEEE Trans. Power Syst.* 31 (6) (2016) 4732–4743.
 - [14] T.J. Overbye, X. Cheng, Y. Sun, A comparison of the ac and dc power flow models for Imp calculations, in: *System Sciences, 2004. Proceedings of the 37th Annual Hawaii International Conference on, IEEE, 2004*, pp. 9–pp.
 - [15] P. Yan, A. Sekar, Analysis of radial distribution systems with embedded series facts devices using a fast line flow-based algorithm, *IEEE Trans. Power Syst.* 20 (4) (2005) 1775–1782.
 - [16] L. Bai, T. Jiang, F. Li, H. Chen, X. Li, Distributed energy storage planning in soft open point based active distribution networks incorporating network reconfiguration and dg reactive power capability, *Appl. Energy* 210 (2018) 1082–1091.
 - [17] S.S. AlKaabi, V. Khadkikar, H. Zeineldin, Incorporating pv inverter control schemes for planning active distribution networks, *IEEE Trans. Sustain. Energy* 6 (4) (2015) 1224–1233.
 - [18] Q. Li, R. Ayyanar, V. Vittal, Convex optimization for des planning and operation in radial distribution systems with high penetration of photovoltaic resources, *IEEE Trans. Sustain. Energy* 7 (3) (2016) 985–995.
 - [19] Y. Xie, X. Chen, Q. Wu, Q. Zhou, Second-order conic programming model for load restoration considering uncertainty of load increment based on information gap decision theory, *Int. J. Electr. Power Energy Syst.* 105 (2019) 151–158.
 - [20] S. Huang, Q. Wu, J. Wang, H. Zhao, A sufficient condition on convex relaxation of ac optimal power flow in distribution networks, *IEEE Trans. Power Syst.* 32 (2) (2017) 1359–1368.
 - [21] P. Siano, Demand response and smart grids-a survey, *Renew. Sustain. Energy Rev.* 30 (2014) 461–478.
 - [22] A. Rabiee, E. Hooshmand, A robust model for optimal allocation of renewable energy sources, energy storage systems and demand response in distribution systems via information gap decision theory, *IET Gener., Transm. Distrib.* 13 (4) (26 February 2019) 511–520, to appear.
 - [23] M. Di Somma, G. Graditi, E. Heydarian-Forushani, M. Shafie-Khah, P. Siano, Stochastic optimal scheduling of distributed energy resources with renewables considering economic and environmental aspects, *Renew. Energy* 116 (2018) 272–287.
 - [24] D. Neves, A. Pina, C.A. Silva, Assessment of the potential use of demand response in dhw systems on isolated microgrids, *Renew. Energy* 115 (2018) 989–998.
 - [25] N. Venkatesan, J. Solanki, S.K. Solanki, Residential demand response model and impact on voltage profile and losses of an electric distribution network, *Appl. Energy* 96 (2012) 84–91.
 - [26] M. Shamshiri, C.K. Gan, R. Omar, Assessment of distribution networks performance considering residential photovoltaic systems with demand response applications, *J. Renew. Sustain. Energy* 9 (4) (2017), 045502.
 - [27] G. Carpinelli, G. Celli, S. Mocci, F. Mottola, F. Pilo, D. Proto, Optimal integration of distributed energy storage devices in smart grids, *IEEE Trans. Smart Grid* 4 (2) (2013) 985–995.
 - [28] S.M. Mohseni-Bonab, A. Rabiee, B. Mohammadi-Ivatloo, S. Jalilzadeh, S. Nojavan, A two-point estimate method for uncertainty modeling in multi-objective optimal reactive power dispatch problem, *Int. J. Electr. Power Energy Syst.* 75 (2016) 194–204.
 - [29] M. Parvania, M. Fotuhi-Firuzabad, M. Shahidehpour, Optimal demand response aggregation in wholesale electricity markets, *IEEE Trans. Smart Grid* 4 (4) (2013) 1957–1965.
 - [30] A. Soroudi, A. Rabiee, A. Keane, Information gap decision theory approach to deal with wind power uncertainty in unit commitment, *Electr. Power Syst. Res.* 145 (2017) 137–148.
 - [31] A. Kavousifard, H. Samet, Consideration effect of uncertainty in power system reliability indices using radial basis function network and fuzzy logic theory, *Neurocomputing* 74 (17) (2011) 3420–3427.
 - [32] P.N. Biskas, D.I. Chatzigiannis, A.G. Bakirtzis, European electricity market integration with mixed market designs-part i: formulation, *IEEE Trans. Power Syst.* 29 (1) (2014) 458–465.
 - [33] M. Amelin, An evaluation of intraday trading and demand response for a predominantly hydro-wind system under nordic market rules, *IEEE Trans. Power Syst.* 30 (1) (2015) 3–12.
 - [34] S. Drewes, S. Ulbrich, *Mixed integer second order cone programming*, Verlag Dr. Hut, 2009.
 - [35] Frontline Systems, Inc, *Linear programming and quadratic programming*, <http://www.solver.com>; accessed 14 May 2018.
 - [36] N. Li, L. Chen, S.H. Low, Exact convex relaxation of opf for radial networks using branch flow model, in: *Smart Grid Communications (SmartGridComm), 2012 IEEE Third International Conference on, IEEE, 2012*, pp. 7–12.
 - [37] L. Gan, N. Li, U. Topcu, S.H. Low, Exact convex relaxation of optimal power flow in radial networks, *IEEE Trans. Autom. Control* 60 (1) (2015) 72–87.
 - [38] K. Deb, *Multi-objective optimization using evolutionary algorithms*, vol. 16, John Wiley & Sons, 2001.
 - [39] J. Meskens, J. Vermeulen, K. Luyten, K. Coninx, Gummy for multi-platform user interface designs: shape me, multiply me, fix me, use me, in: *Proceedings of the working conference on Advanced visual interfaces, ACM, 2008*, pp. 233–240.
 - [40] Gurobi Optimization, Inc, *Gurobi optimizer reference manual*, <http://www.gurobi.com> (Online; accessed 14 July 2018).